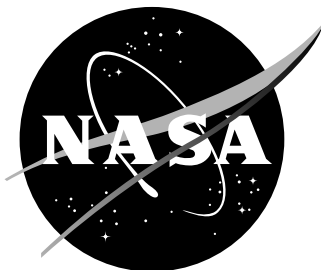


Ames Research Center
Moffett Field, California 94035

Technical Support Package

Direct Time Integration of Maxwell's Equations

NASA Tech Briefs
ARC-13259



National Aeronautics and
Space Administration

Technical Support Package

for

DIRECT TIME INTEGRATION OF MAXWELL'S EQUATIONS

ARC-13259

NASA Tech Briefs

The information in this Technical Support Package comprises the documentation referenced in **ARC-13259** of *NASA Tech Briefs*. It is provided under the Technology Transfer Program of the National Aeronautics and Space Administration to make available the results of aerospace-related developments considered to have wider technological, scientific, or commercial applications. Further assistance is available from sources listed in *NASA Tech Briefs* on the page entitled "NASA Commercial Technology Team."

Additional information regarding research and technology in this general area may be found in Scientific and Technical Aerospace Reports (STAR), which is a comprehensive abstracting and indexing journal covering worldwide report literature on the science and technology of space and aeronautics. STAR is available to the public on subscription from

Registration Services
NASA Center for AeroSpace Information
800 Elkridge Landing Road
Linthicum Heights, MD 21090-2934

Telephone: (301) 621-0390, Fax: (301) 621-0134, E-mail: help@sti.nasa.gov

NOTICE: This document was prepared under the sponsorship of the National Aeronautics and Space Administration. Neither the United States Government nor any person acting on behalf of the United States Government assumes any liability resulting from the use of the information contained in this document or warrants that such use will be free from privately owned rights.

Direct Time Integration of Maxwell's Equations in Nonlinear Dispersive Media for Propagation and Scattering of Femtosecond Electromagnetic Solitons

Peter M. Goorjian, NASA, Ames Research Center, Moffett Field, California
and
Allen Taflove, Department of Electrical Engineering and Computer Science, McCormick School
of Engineering, Northwestern University, Evanston, Illinois

A. ABSTRACT

We report the initial results for femtosecond electromagnetic soliton propagation and collision obtained from first principles, i.e., by a direct time integration of Maxwell's equations. The time integration efficiently implements linear and nonlinear convolutions for the electric polarization and can take into account such quantum effects as Kerr and Raman interactions. The present approach is robust and should permit the modeling of two- and three-dimensional optical soliton propagation, scattering, and switching from the full-vector Maxwell's equations.

B. DISCUSSION

This Letter introduces a direct solution to Maxwell's vector-field equations suitable (in principle) for modeling the propagation and scattering of optical pulses, including solitons, in inhomogeneous nonlinear dispersive media. We believe that this approach will eventually provide a modeling capability for millimeter-scale integrated optical circuits beyond that of existing techniques that use the generalized nonlinear Schrödinger equation (GNLSE).

In Ref. 1, we discussed an efficient finite-difference time-domain (FD-TD) numerical approach for the direct time integration of Maxwell's equations to model linear media that have arbitrary-order chromatic dispersions. The approach was based on a suggestion by Jackson² to relate $D(t)$ to $E(t)$ with an ordinary differential equation in time integrated concurrently with the Maxwell equations. In this manner, we computed reflection coefficients accurate to better than 6 parts in 10,000 over the frequency range of dc to 3×10^{16} Hz for a single 0.2-fs Gaussian pulse incident upon a Lorentz half-space and obtained new results for the Sommerfeld and Brillouin precursors.

In this Letter, we report a generalization of the above to deal with the nonlinear terms of the electric polarization. The FD-TD direct time integration of Maxwell's equations can now incorporate nonlinear instantaneous and nonlinear dispersive effects as well as linear dispersive effects, thereby permitting the modeling of optical solitons that have large instantaneous bandwidths.

We again consider a one-dimensional problem with field components E_z and H_y , propagating in the x direction. Assuming that the medium is nonpermeable and isotropic, we see that Maxwell's equations in one dimension are written as

$$\frac{\partial H_y}{\partial t} = \frac{1}{\mu_0} \frac{\partial E_z}{\partial x}, \quad (1a)$$

$$\frac{\partial D_z}{\partial t} = \frac{\partial H_y}{\partial x}, \quad (1b)$$

$$E_z = \frac{D_z - (P_{z_L} + P_{z_{NL}})}{\epsilon_0}. \quad (1c)$$

Here we assume that the polarization consists of two parts: a linear part P_{z_L} and a nonlinear part

$P_{z_{NL}}$. P_{z_L} is given by a linear convolution of $E_z(x,t)$ and the susceptibility function $\chi^{(1)}$,

$$P_{z_L}(x,t) = \epsilon_0 \int_{-\infty}^{\infty} \chi^{(1)}(t-t') E_z(x,t') dt', \quad (2a)$$

and $P_{z_{NL}}$ is given by a nonlinear convolution of $E_z(x,t)$ and the third-order susceptibility $\chi^{(3)}$,

$$P_{z_{NL}}(x,t) = \epsilon_0 \int_{-\infty}^{\infty} \int_{-\infty}^{\infty} \int_{-\infty}^{\infty} \chi^{(3)}(t-t_1, t-t_2, t-t_3) \times \\ E_z(x,t_1) E_z(x,t_2) E_z(x,t_3) dt_1 dt_2 dt_3. \quad (2b)$$

This provides the physics of a nonlinearity with time retardation or memory, i.e., a dispersive nonlinearity that can occur because of quantum effects in silica at time scales of 1-100 fs. Note that $\chi^{(3)}$ may differ from $\chi^{(1)}$ in physical properties such as resonances and dampings.

We consider a material having a Lorentz linear dispersion characterized by the following $\chi^{(1)}$:

$$\begin{aligned}\chi^{(1)}(t) &= \frac{\omega_p^2}{\nu_0} e^{-\delta t/2} \sin \nu_0 t \\ &= F^{-1}[\chi^{(1)}(\omega)] \\ \rightarrow \epsilon(\omega) &= \epsilon_\infty + \frac{\omega_0^2(\epsilon_s - \epsilon_\infty)}{\omega_0^2 - j\delta\omega - \omega^2},\end{aligned}\tag{3}$$

where $\omega_p^2 = \omega_0^2(\epsilon_s - \epsilon_\infty)$ and $\nu_0^2 = \omega_0^2 - \delta^2/4$. Further, the material nonlinearity is assumed to be characterized by the nonlinear single time convolution for $P_{z_{NL}}$,⁴

$$P_{z_{NL}}(x,t) = \epsilon_0 \chi^{(3)} E_z(x,t) \times \int_{-\infty}^{\infty} [\alpha \delta(t-t') + (1-\alpha) g_R(t-t')] E_z^2(x,t') dt'. \tag{4}$$

Here $\chi^{(3)}$ is the nonlinear coefficient, $\delta(t)$ models Kerr nonresonant virtual electronic transitions on the order of about 1 fs or less, $g_R(t) = [(\tau_1^2 + \tau_2^2)/\tau_1 \tau_2^2] e^{-t/\tau_2} \sin(t/\tau_1)$ and models transient Raman scattering, and α parameterizes the relative strengths of the Kerr and Raman interactions. Effectively, $g_R(t)$ models a single Lorentzian line that is centered on the optical phonon frequency $1/\tau_1$ and has a bandwidth of $1/\tau_2$ (the reciprocal phonon lifetime).

We now describe a system of coupled nonlinear ordinary differential equations to characterize the physics of Equations (3) and (4). Assuming zero initial conditions at $t = 0$, we define the functions $F(t)$ and $G(t)$, respectively, as the linear and nonlinear convolutions,

$$F(t) = \varepsilon_0 \int_0^t \chi^{(1)}(t-t') E_z(x,t') dt', \quad (5)$$

$$G(t) = \varepsilon_0 \int_0^t g_R(t-t') E_z^2(x,t') dt'. \quad (6)$$

Then, F and G satisfy the following coupled system of nonlinear ordinary differential equations:

$$\begin{aligned} \frac{1}{\omega_0^2} \frac{d^2 F}{dt^2} + \frac{\delta}{\omega_0^2} \frac{dF}{dt} + \left[1 + \frac{\varepsilon_s - \varepsilon_\infty}{\varepsilon_\infty + \alpha \chi^{(3)} E^2} \right] F + \\ \frac{(\varepsilon_s - \varepsilon_\infty)(1 - \alpha) \chi^{(3)} E G}{\varepsilon_\infty + \alpha \chi^{(3)} E^{(2)}} = \frac{(\varepsilon_s - \varepsilon_\infty) D}{\varepsilon_\infty + \alpha \chi^{(3)} E^2}, \end{aligned} \quad (7)$$

$$\begin{aligned} \frac{1}{\omega_0^2} \frac{d^2 G}{dt^2} + \frac{\bar{\delta}}{\omega_0^2} \frac{dG}{dt} + \left[1 + \frac{(1 - \alpha) \chi^{(3)} E^2}{\varepsilon_\infty + \alpha \chi^{(3)} E^2} \right] G + \\ \frac{EF}{\varepsilon_\infty + \alpha \chi^{(3)} E^{(2)}} = \frac{DE}{\varepsilon_\infty + \alpha \chi^{(3)} E^2}, \end{aligned} \quad (8)$$

where $\bar{\delta} = 2/\tau_2$ and $\bar{\omega}_0^2 = (1/\tau_1)^2 + (1/\tau_2)^2$. Equations (7) and (8) are first solved simultaneously for F and G at the latest time step by using a second-order-accurate finite-difference scheme that operates on data for the current value of D and previous values of D , E , F , and G . Only two time levels of storage are required with this approach. Then, the latest value of E can be obtained by means of Newton's iteration of the following equation, using the new values of D , F , and G :

$$E = \frac{D - F - (1 - \alpha) \chi^{(3)} E G}{\varepsilon_0 (\varepsilon_\infty + \alpha \chi^{(3)} E^2)}. \quad (9)$$

The algorithm for the system of Equations (7), (8), and (9) is inserted to implement Equation (1c). This, combined with the usual FD-TD realization of Equations (1a) and (1b),¹ makes up the complete solution method.

We now demonstrate the integration of Maxwell's equations to obtain soliton dynamics. A pulsed optical signal source is assumed to be located at $x = 0$. The pulse is assumed to have unity amplitude of its sinusoidal-carrier electric field, a carrier frequency $f_c = 1.37 \times 10^{14}$ Hz ($\omega_c = 8.61 \times 10^{14}$ rad/s), and a hyperbolic-secant envelope function with a characteristic time constant of 14.6 fs. Approximately seven cycles of the carrier are contained within the pulse envelope, and the center of the pulse coincides with a zero crossing of the sinusoid. To achieve soliton formation over short propagation spans of less than 200 μm , we scale values of group-velocity dispersion β_2 and nonlinear coefficient $\chi^{(3)}$. For example, let $\epsilon_s = 5.25 \epsilon_0$, $\epsilon_\infty = 2.25 \epsilon_0$, $\omega_0 = 4.0 \times 10^{14}$ rad/s, $\delta = 2.0 \times 10^9 \text{ s}^{-1}$, $\chi^{(3)} = 7 \times 10^{-2} (\text{V/m})^{-2}$, $\alpha = 0.7$, $\tau_1 = 12.2$ fs, and $\tau_2 = 32$ fs. (The last three values are from Ref. 4.) This results in β_2 varying widely over the spectral width of the pulse; i.e., from -7 to -75 ps^2/m over the range $(1.37 \pm 0.2) \times 10^{14}$ Hz. Finally, by choosing a uniform FD-TD space resolution of 5 nm ($\approx \lambda_0/300$), the numerical phase velocity error is limited to approximately 1 part in 10^5 , small compared with that of the physical dispersions being modeled.

Figure 1 depicts the FD-TD computed propagating pulse for the linear case [$\chi^{(3)} = 0$] observed at $n = 2 \times 10^4$ and 4×10^4 time steps, corresponding to propagation to $x = 55 \mu\text{m}$ and $126 \mu\text{m}$. Note pulse broadening, diminishing amplitude, and carrier frequency modulation ($> f_c$ on the leading side and $< f_c$ on the trailing side), which cause an asymmetrical shifting of the envelope, a higher-order dispersive effect. These qualitative features of the effect of anomalous dispersion have been predicted⁵ but until now have not been computed by directly integrating Maxwell's equations.

In Figure 2, we set $\chi^{(3)} = 7 \times 10^{-2} (\text{V/m})^{-2}$, which yields a soliton that retains its amplitude and width. However, a second, low-amplitude soliton is seen to move out and ahead of the main soliton. The carrier frequency of this daughter soliton is upshifted to $\approx 4.9 \times 10^{14}$ Hz, approximately 3.6 times that of the main soliton. From GNLSE theory, the appearance of the daughter soliton is predicted because of the assumed higher-order dispersive and nonlinear effects.³ However, GNLSE theory does not easily predict the carrier frequency shift that we have

computed for this pulse. Also, in both cases depicted in Figures 1 and 2, by observing a video of the pulse evolution, it was noted that the phase velocity of the carrier was substantially greater than the group velocity of the envelope.

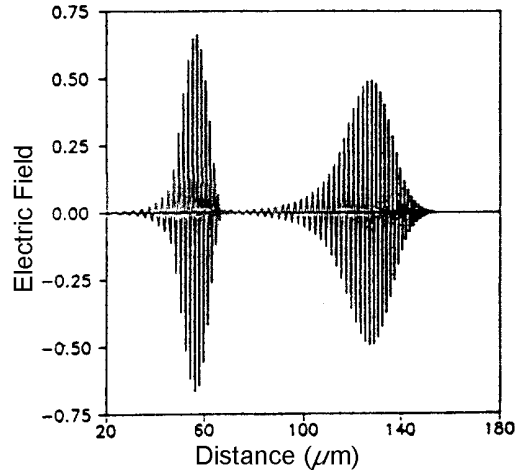


Figure 1

Finite-difference time-domain results for the optical carrier pulse (linear case) after it has propagated 55 μm and 126 μm in the Lorentz medium.

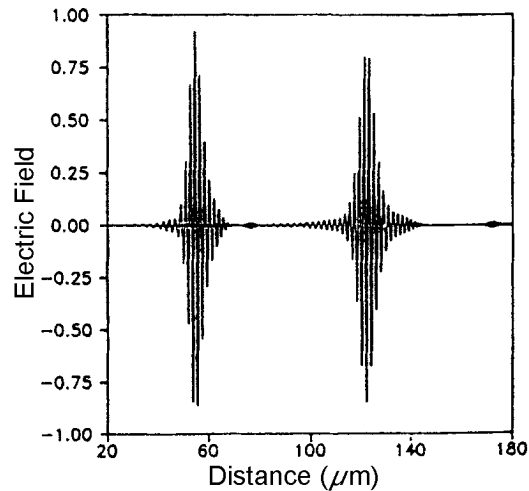


Figure 2

Finite-difference time-domain results for the optical soliton carrier pulse that correspond to the observation locations of Figure 1.

Figure 3 depicts the Fourier spectrum of the main solitons shown in Figure 2. The figure shows a 4-THz red shift and a sharpening of the spectrum as the pulse propagates. From GNLSE theory,

the red shift is predicted because of the Raman effect's^{3,4} occurring as a higher-order dispersive nonlinearity modeled by the function $g_R(t)$ in the kernel of Equation (4).

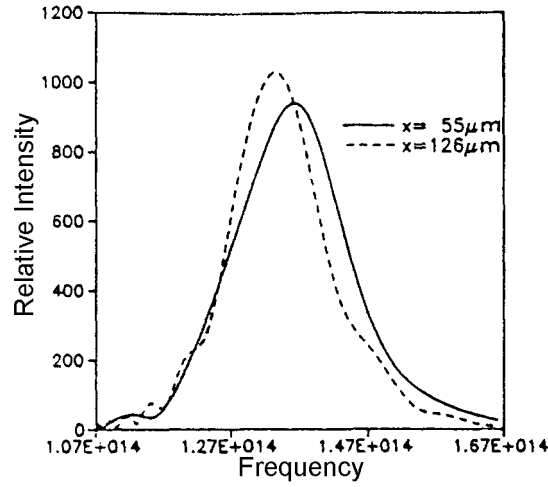


Figure 3

Red shift of the Fourier spectrum of the main propagating soliton of Figure 2.

Last, we consider the collision of two counter-propagating solitons. They are identical and have all the parameters of the above case. As is characteristic of colliding solitons,⁶ after the collisions, both main and daughter pulses separate and move apart without changing their general appearances. However, there are lagging phase shifts due to the collision: 12° for the carrier in the main solitons and 31° for the carrier in the daughters. To illustrate this, in Figure 4 we plot the space dependence of the central part of the rightward-moving daughter for the original uncollided case and the collided case, with both curves at exactly 30,000 time steps of the algorithm. Such phase shifts, not easily detected by GNLSE, may be a basis for optical switching devices.

The approach of this Letter assumes nothing about the homogeneity or isotropy of the optical medium, the magnitude of its nonlinearity, the nature of its ω - β variation, and the shape or duration of the optical pulse. By retaining the optical carrier, the new method solves for fundamental quantities, the optical electric and magnetic fields in space and time, rather than a nonphysical envelope function. Thus it is extendable to full-vector optical fields in two and three dimensions to permit rigorous boundary-value problem studies of nonlinear vector-wave polarization, diffraction, scattering, and interference effects.

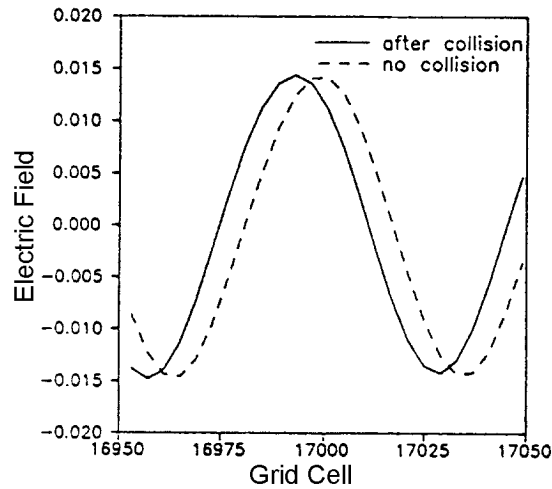


Figure 4

Phase lag of the rightward-moving daughter soliton as a result of collisions with counter-propagating solitons.

The author acknowledges the assistance of Rose Joseph in this research, including many helpful discussions, performance of some of the calculations, and preparation of the figures. A. Taflove was supported in part by NASA-Ames University Consortium Joint Research Interchange grants NCA2 561 and 562, Office of Naval Research contract N00014-88-K-0475, and Cray Research, Inc.

REFERENCES

1. Joseph, R.M., Hagness, S.C., and Taflove, A., *Opt. Lett.* **16**, 1412, 1991.
2. Jackson, J.D., *Classical Electrodynamics*, 2nd ed., Wiley, New York, 1975.
3. Agrawal, G.P., *Nonlinear Fiber Optics*, Academic, New York, 1989.
4. Blow, K.J., and Wood, D., *IEEE, J. Quantum Electron.*, **25**, 2665 1989.
5. Bell, T.E., *IEEE Spectrum*, **27**(8), 56, 1990.
6. Marcuse, D., *Theory of Dielectric Optical Waveguides*, 2nd ed., Academic, New York, 1991.